JOURNAL OF APPLIED ELECTROCHEMISTRY 20 (1990) 596–605

Electrodeposition of polypyrrole layers on aluminium from aqueous electrolytes

P. HÜLSER, F. BECK

University of Duisburg, FB 6-Elektrochemie, Lotharstrasse 1, D-4100 Duisburg 1, FRG

Received 3 July 1989; revised 19 October 1989

A screening of twenty aqueous electrolytes for a film-forming electropolymerization of pyrrole with Al was performed. Electrodeposition of well adhering homogeneous polypyrrole layers on aluminium is possible from aqueous electrolytes containing 0.1–0.8 M oxalic acid. Pretreatment of the metal by polishing (PD) or by anodic (galvanostatic) activation (GA) is an essential step. In all cases, the Al_2O_3 surface layer with pores, usually filled with electrolyte, is transformed to a Al_2O_3 layer with polypyrrole filled pores. The PPy-layers on Al allow an easy cathodic coating with metals like copper. The hydrogenoxalate doped layers exhibit the ususal redox capacity, $y = 0.3$. The sandwich structure $Al/Al_2O_3/PPy$ represents a condenser with an unusual composite dielectric with the electronically conducting 'plates' Al and PPy. According to our impedance measurements, the PPy *in the pores* is a high resistivity material due to overoxidation in the course of electropolymerization at high local current densities. The composite, Al_2O_3/overoxidized PPy, exhibits an unusually high permittivity, in the order of 10^3.

1. Introduction

Chemical oxidation of pyrrole with H_2O_2, $FeCl_3$ or quinones affords a precipitation of polypyrrole powder (pyrrole black) [1, 2]. Also direct anodic oxidation of the monomer in aqueous sulphuric acid on platinum leads to black coatings of polypyrrole [3, 4]. A large improvement in quality and reversible redox capacity of the polypyrrole layers was accomplished by Diaz *et al.*, who employed salts like NBu_4BF_4 or $LiClO_4$ in acetonitrile (with ~ 1% H_2O) as a solvent/electrolyte-system [5, 6]. Electrocoatings of polypyrrole and other conducting polymers have been widely investigated and, almost exclusively, inert anodes like Pt, Au or glassy carbon (GC) have been used [7–9]. Only in a few cases were other anode substrates investigated, namely, evaporated metal films [10], sheets of Fe, Al, brass and Ti [11] and of Fe, stainless steel, Cu and Ti [12]. From a practical point of view, commodity metals like iron or aluminium, predominantly in combination with aqueous electrolytes, should be highly interesting. Interference of their anodic active/passive behaviour with the anodic electrolpolymerization process to yield a new adhering polymer phase is expected. In the present paper, we report on a systematic study of aqueous electrolytes for the electrocoating of aluminium. Our results in nonaqueous electrolytes will be published elsewhere [13].

2. Experimental details

Pyrrole (Merck, zur Synthese) was freshly distilled under nitrogen. Concentrations between 0.1 and 1 M were used. The electrolytes (AnalaR quality) were dissolved in triple distilled water. Aluminium sheets (0.1 mm) were employed as strips partially coated with a special self-adhering PVC tape; they had an accessible free area of 2 or 4 cm^2 [14]. The metal (from Riedel de Haen) was usually 99.5% pure (0.2% Fe, 0.2% Si, 0.1% others). Control measurements were performed with 99.997% Al (Johnson Matthey).

After degreasing the Al in tetrachloroethylene for half an hour, two further pretreatment methods were employed alternatively. These were: polishing with diamond spray (6 μm) at a rotating textile disk (PD); and galvanostatic activation in 0.1 M HNO_3/0.1 M pyrrole at 24 mA cm^{-2} for 2 minutes (GA). Thereafter, the Al sheet was thoroughly rinsed with distilled water, and also with acetone in the case of PD.

The electrochemical cell had the usual three electrode configuration. The potentials, U_{SSCE}, were measured with respect to a NaCl saturated calomel electrode, which is + 236 mV with respect to SHE. Voltammetric measurements, mostly at 2 mV s^{-1}, were performed with a potentiostat (Wenking CT 73), a voltage scan generator (Wenking VSG 72) and an XY-recorder (Rohde and Schwarz ZSK 2). Galvanostatic electrodepositions (galvanostat AMEL 545) were run at 0.2–5 mA cm^{-2} in slowly stirred electrolytes. In some cases, larger Al-sheets of 42 cm^2 free surface were employed. The counter electrodes were of stainless steel in these cases.

Impedance measurements were performed in the frequency range 0.1–10^5 s^{-1}. A Solartron frequency response analyzer (HF 1255) in combination with a PAR (EG & G) potentiostat 273 were employed. If not stated otherwise, all electrochemical operations were performed under nitrogen at 20° C.

0021-891X/90 $03.00 + .12

Table 1. Current-voltage data for three categories of electrolytes, (see Fig. 1 and text). 0.1 M electrolyte, with or without 0.1 M pyrrole, at 20° C, 2 mV s^{-1}, Al-pretreatment PD

Category	*Electrolyte*	*j(mA cm^{-2}) at U_{SSCE} = 0.85 V*		*U_{SSCE} (V) at 1 mA cm^{-2}*		*PPy layer*
		with Py	*without Py*	*with Py*	*without Py*	
A	HNO_3	1.60	0.20			+
	HOOC–COOH	1.15	0.17			+
Electrodeposition	H_2SO_4	1.0*	0.25			+
of PPy	H_3PO_4	0.75†	0.33†			+
	NEt_4HSO_4	1.0‡	0.18			+
B	NaCl			−0.68	−0.68	−
Active dissolution of	NaBr			−0.54	−0.54	−
Al with the formation	$NaClO_4$			−0.21	−0.22	−
of pits	NBu_4PTS			0.07	0.07	−
	$NaBF_4$			0.55	0.55	−
	CH_3SO_3H			0.76	0.76	−
	KSCN			1.80	1.80	−
	KNO_3			1.79	1.77	−
C	CH_3COOH	0.05	0.05			−
Passive behaviour	$NaHCO_3$	0.05	0.05			−
	H_3BO_3	0.25	0.20			−
	NaH_2PO_4	0.25	0.25			−

PTS = p-toluenesulphonate.
*700 mV/0.8 M pyrrole.
† 0.8 M pyrrole, U_{SSCE} = 1.0 V.
‡ 0.8 M pyrrole.

3. Results and discussion

3.1. *Cyclovoltammetric screening*

Potentiodynamic current voltage curves up to U_{SSCE} = 2 V were measured in the absence and in the presence of pyrrole. The aluminium was pretreated according to PD. As seen in Table 1, three categories of electrolytes can be distinguished. Only with some acid electrolytes (category A), could a coherent, adhering polypyrrole layer be observed. The electrolytes have been known for a long time as a medium for uniform etching of the Al and sulphuric acid, oxalic acid and phosphoric acid are suitable for the anodic formation of a thickened Al_2O_3-layer with a duplex structure at relatively low potentials [15, 16]. A homogeneous chemical dissolution of the Al_2O_3 layer leads, on the other hand, to an appreciable thinning of the passive

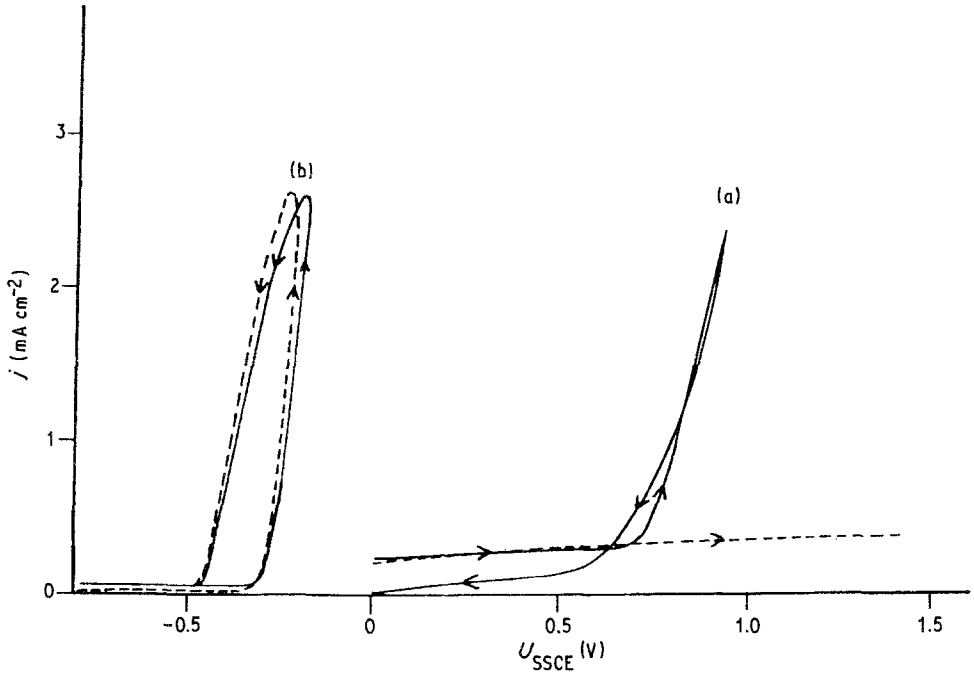

Fig. 1. Voltammetric curves (2 mV s^{-1}) of the potentiodynamic electrodeposition of polypyrrole on aluminium (polished PD), in aqueous solution, no stirring, 20° C. Curve (a): 0.1 M $H_2C_2O_4$; Curve (b): 0.1 M $NaClO_4$. —— in the presence of 0.1 M pyrrole; – – – basic curve without pyrrole.

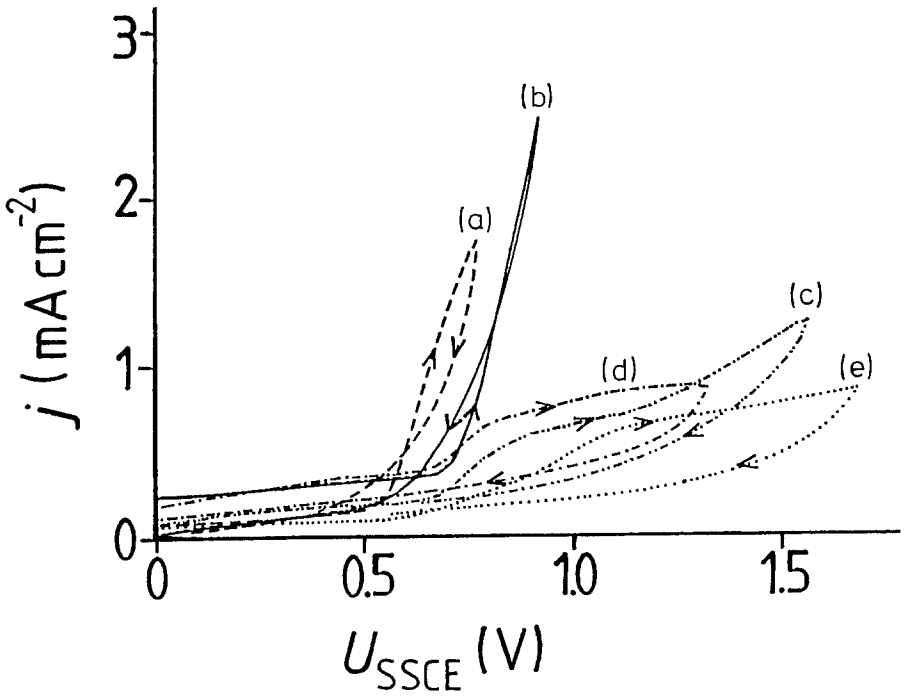

Fig. 2. Voltammetric curves ($2\,mV\,s^{-1}$) of the potentiodynamic electrodeposition of polypyrrole on different pretreated aluminium in aqueous solution (0.1 M $H_2C_2O_4$, 0.1 M pyrrole), no stirring, 20° C. Curve (a), – – –, anodic activation (GA); Curve (b), ——, polishing (PD); Curve (c), – – –, etching in 10% NaOH, 50° C, 2.5 min.; Curve (d), –·–·–·–, as curve c, but with subsequent etching (2 min.) in 10% HNO_3 after intermediate rinsing with distilled water; Curve (e), ····, unpretreated, degreased only.

film. The basic currents in the absence of pyrrole are relatively high. In the presence of pyrrole, the current rises strongly at potentials which are a few 100 mV more positive than those where the polymer is formed at platinum. This is due to the voltage drop in the barrier layer. Table 1 (category A) reveals that for H_2SO_4 and H_3PO_4 a higher pyrrole concentration (0.8 M) is necessary to yield a homogeneous PPy layer. With 0.1 M pyrrole, as in the case of oxalic acid and HNO_3, no pronounced current rise like that in Fig. 1, curve (a) could be detected. Fig. 1, curve (a) demonstrates an example with oxalic acid. As shown in Fig. 2, a mechanical pretreatment (PD) (see § 2) is also necessary in order to partially remove the 'old', relatively inactive, Al_2O_3 layer. We assume a predominant polypyrrole deposition at the bottom of the pores in the duplex layers, that is, at the surface of the coherent primary oxide film, see Fig. 11a. As the diameters of these pores are only of the order of 30 nm, we were not able to distinguish directly the early stages of this electrodeposition. Due to the high density of these pores, ($10^{10}\,cm^{-2}$), the adhesion of the electrodeposited PPy-layers is excellent.

The electrolytes of category B, mainly neutral salts, lead to an active dissolution of aluminium at relatively negative potentials. The anodic dissolution concentrates in pits which are initiated at the oxide layer [17–20]. The pit diameter is of the order of 10–30 μm, the number of pits increases with the geometric current density. The relatively defined 'pitting potential', where a steep rise of current density is noticed, corresponds to the observations of other experimenters [19–21]. Fig. 1b shows $NaClO_4$ as an example. In spite of the very positive pitting potential for KSCN and KNO_3, virtually no PPy was formed (in the pits) under the conditions of Table 1. However, at higher pyrrole concentrations (0.8 M), some electropolymerization was observed in the case of KSCN. Therefore, this must be regarded as a borderline case with respect to category A. Starting from unpolished Al and 0.1 M HNO_3 as an electrolyte, originally discussed in category A in connection with Al pretreated by method PD, the pitting potential of 1.77 V could be attained under galvanostatic (GA) or potentiodynamic polarization. PPy deposits were observed in the pits, cf. § 4. With 99.997% Al as a substrate, essentially the same current/voltage and pitting behaviour could be observed under these conditions. Thus, pitting is governed by the electrolyte and by the potential rather than by the purity of the aluminium.

Finally, all electrolytes belonging to category C only show a pronounced passive behaviour up to $U_{SSCE} = 2\,V$. The corrosion current densities are relatively low in most cases.

3.2. *Influence of pretreatment of aluminium*

It has already been mentioned in the previous section that the mode of pretreatment of the metal strongly influences the subsequent electrochemical formation of PPy layers. Fig. 2 shows some typical examples. Polishing with diamond paste (PD) or galvanostatic (or potentiodynamic) activation into the pitting region (GA) seem to be essential steps prior to the electrodeposition. Etching, or only degreasing of the Al sheets, led to a distorted current-voltage behaviour. Thus repassivation occurred after the chemical etch. Only after the first two methods of pretreatment,

was a coherent and adherent layer of smooth PPy deposited, while in the other three cases only a thin non-perfect coating was observed.

3.3. *Galvanostatic deposition after mechanical pretreatment (PD)*

This kind of electrodeposition was performed as a parametric study. Larger Al sheets of 42 cm^2 area were employed to improve the accuracy of mass difference determination. Table 2 displays some characteristic results. Nominal thickness, d_n, and current efficiency, c.e., are defined in [12]. The degree of insertion, from elemental analysis of the product No. 6 in Table 2, appears to be about 0.2, assuming the oxygen content (100 − (C + H + N) %) to be due to the overall composition $(C_4H_3N) \cdot (0.18 \ldots 0.21)\, HC_2O_4^- \cdot 2H_2O$.

An increasing *pyrrole concentration* (entries 1–4) has the following consequences: transition from an erratic deposition, predominantly along scratches, at 0.1 M pyrrole to a homogeneous PPy layer at the higher concentrations. The current efficiency increases from 56 to 84%. The working potential decreases from 900 to 540 mV. The same was observed in the course of electrode kinetic investigations [22, 23]. The potential at the lowest concentration is not stable, but tends to increase during the course of the electrodeposition process, see Fig. 3. This is readily explained as a growth of the Al_2O_3 layer in parallel to the polypyrrole formation due to the positive potential. At higher pyrrole concentrations, the electropolymerization itself is favoured, and the polymerization protects the Al substrate even in the early stages of the process. Table 2 clearly shows that a maximum current efficiency is obtained with *oxalic acid electrolyte*, cf. Nos. 1, 12 and 13. It should be noted that the anodic decomposition of oxalic acid proceeds at similar

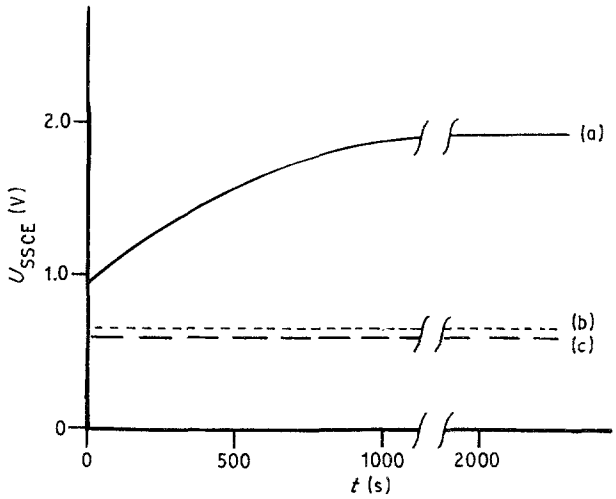

Fig. 3. Galvanostatic deposition of polypyrrole on aluminium (polished) in aqueous solution (0.1 M $H_2C_2O_4$) at various pyrrole concentrations, $j = 0.5\,mA\,cm^{-2}$ (stirring, 20° C). Curve (a), ——, 0.1 M pyrrole; Curve (b), – – –, 0.4 M pyrrole, Curve (c), — —, 0.8 M pyrrole. $d_n = 3\,\mu m$.

potentials. Even with platinum, the anodic decomposition of the electrolyte and the electrodeposition of PPy with simultaneous doping of the polymer with hydrogenoxalate proceed at nearly the same potential. Nevertheless, in the presence of pyrrole, electropolymerization prevails, and the electrolyte decomposition is only indicated by a few bubbles of CO_2. Another important parameter is the *temperature* of electrodeposition (entries 5–11). Lower temperatures are advantageous and, at 0° C, the best results, smooth, strongly adherent PPy layers, were obtained from 0.8 M PPy/0.1 M oxalic acid. The *current density* is the last parameter to be discussed. Table 2 shows nearly invariant current efficiencies in the range 0.5–5 $mA\,cm^{-2}$.

Table 2. Electrodeposition of PPy on Al at constant current densities, j, after mechanical PD. Electrolyte concentration = 0.1 M. Nominal thickness $d_n = 3\,\mu m$

No.	*Electrolyte*	$c_{pyrrole}$ (*M*)	*j* ($mA\,cm^{-2}$)	*T* (° *C*)	*c.e.* (%)	*Working potential* U_{SSCE} (*mV*)
1	HOOC–COOH	0.1	0.5	20	56	900–2100
2		0.4	0.5	20	76	650
3		0.8	0.5	20	84	600
4		1.0*	0.5	20	83	540
5		0.8	0.5	20	88†	550
6		0.8	0.5	15	90	585
7		0.8	1.0	15	94	610
8		0.8	1.0	0	94/99‡	610
9		0.8	2.0	0	94/94‡	640
10		0.8	2.5	0	95	700
11		0.8	5.0	0	91	4000–4800
12	H_2SO_4	0.1	0.5	20	40	1000–3000
13	HNO_3	0.1	0.5	20	37	1700–1000
14		0.4	0.5	20	45	600–500

* Emulsion.
† Pt anode.
‡ $d_n = 10\,\mu m$.

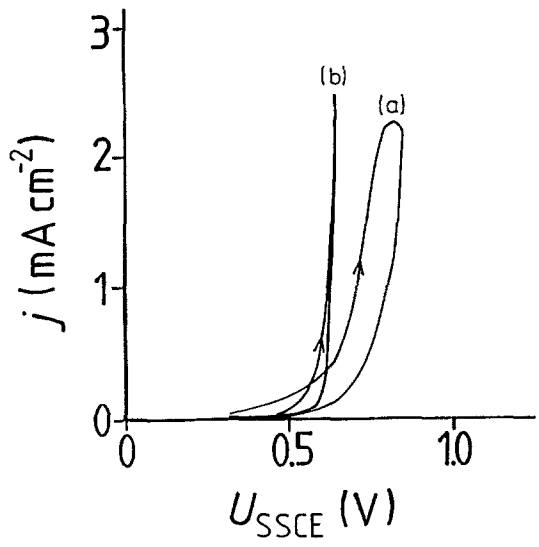

Fig. 4. Potentiodynamic oxidation of oxalic acid at platinum ($2\,mV\,s^{-1}$, 20° C, no stirring). Curve (a): 0.1 M oxalic acid; Curve (b): as (a), but with 0.1 M pyrrole in addition.

Table 3. Electrodeposition of PPy on Al at constant current densities, j, after anodic pretreatment GA. Electrolyte concentration = 0.1 M. Nominal thickness d_n = 3 μm

No.	*Electrolyte*	$c_{pyrrole}$ (*M*)	*j* ($mA\,cm^{-2}$)	*c.e.* (%)
1	HOOCH–COOH	0.1	0.5	63
2		0.8	0.3	82
3		0.8	0.5	88
4		0.8	0.5	78*
5		0.8	1.0	89
6		0.8	2.0	98
7	H_2SO_4	0.8	0.5	68
8		0.8	1.0	74
9	HNO_3	0.4	1.0	powdery deposit

* Anodic activation GA in the absence of pyrrole.

3.4. *Galvanostatic deposition after anodic pretreatment (GA)*

Anodic activation of the Al substrate can be performed galvanostatically at high current densities in 0.1 M HNO_3/0.1 M pyrrole (for instance, pretreatment mode GA in § 2, and Fig. 5). The pitting potential of Al at 2 V with respect to SHE in the presence of NO_3^- is attained, and the formation of pits, partially filled with PPy, sets in. Al dissolves anodically with nearly quantitative current efficiency.

If, after such a pretreatment, the anodic polarization is continued at low current densities and high pyrrole concentrations, predominantly in 0.1 M oxalic acid, a strongly adherent, smooth, coherent PPy coating is electrodeposition. Fig. 5 demonstrates the negative shift of the potential. Table 3 lists some current efficiencies, demonstrating that they are, in some cases, even higher than the corresponding values in Table 2. Table 3 also shows that activation in the absence of pyrrole leads to inferior results, for the nucleation of PPy must proceed in the second phase, in competition with further Al dissolution. H_2SO_4 as an electrolyte leads to lower current efficiencies and irregular electrodeposits.

A potentiodynamic activation of Al ($2\,mV\,s^{-1}$) in 0.1 M HNO_3 is possible too. The anodic current rises steeply at 1.8 V vs SSCE, and pitting occurs again. In the presence of pyrrole, the pits are filled with polypyrrole. This is a favoured pretreatment for the electrodeposition of polypyrrole-*powder*, on which we shall report elsewhere [24, 25].

3.5. *Redox capacity of the Al/PPy-system*

Electrodeposition of polypyrrole from oxalic acid electrolyte leads to a doped polymer layer, the dopant presumably being the hydrogen oxalate anion. Fig. 6 gives results for the potentiodynamic electrodeposition on to Al (Q_0) and the first discharge ($Q_{E,0}$) in the conventional electrolyte with 0.1 M NBu_4BF_4 and 0.03 M H_2O in acetonitrile. From such experiments a degree of doping, *y*, of about 30% is calculated by

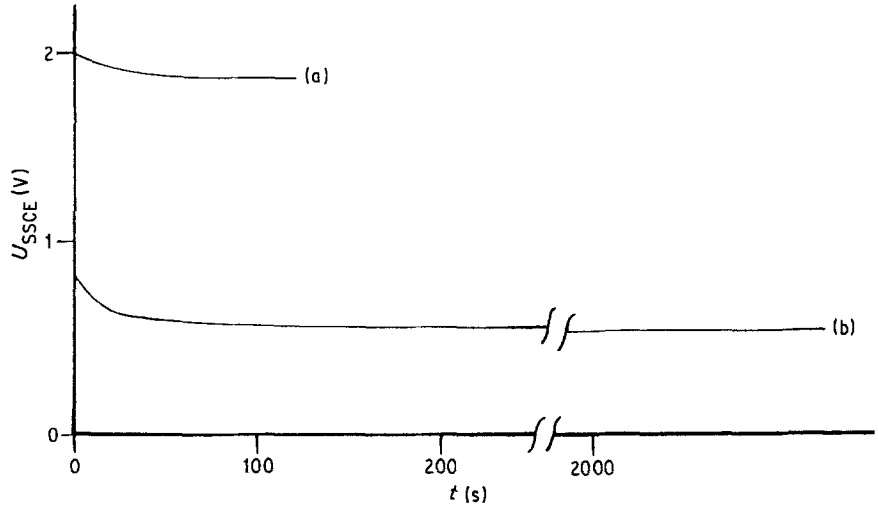

Fig. 5. Potential-time curves for the galvanostatic polarization of Al. Curve (a) 'Galvanostatic activation' (GA) of Al, unpretreated, $j = 25\,mA\,cm^{-2}$, $t = 2$ min, 20° C, 0.1 M HNO_3/0.1 M pyrrole; Curve (b): galvanostatic deposition of polypyrrole on Al, pretreated according to (a) 'GA', $j = 0.5\,mA\,cm^{-2}$, $t = 37.5$ min, 20° C, 0.1 M $H_2C_2O_4$/0.8 M pyrrole, d_n = 3 μm.

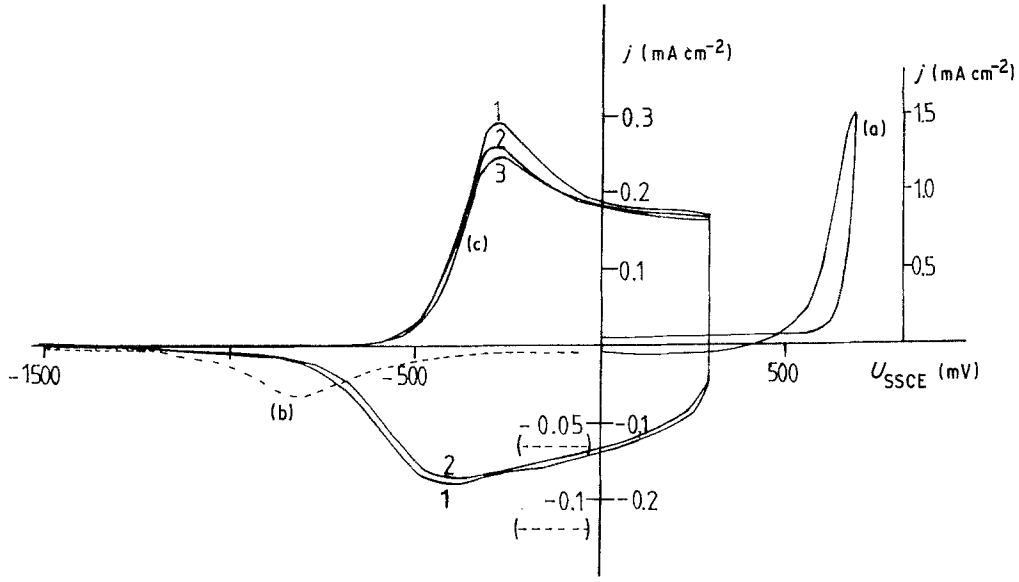

Fig. 6. Redox capacity of PPy layers (d_n = 0.21 μm) on Al. Curve (a): potentiodynamic electrodepostion from 0.1 M oxalic acid/0.8 M pyrrole, 0° C, v_S = 2 mV s^{-1}. Al was pretreated 'PD'. Curve (b): First discharge, 2 mV s^{-1}, 0.1 M NBu_4BF_4, free of bromide, 0.03 M H_2O in CH_3CN, 20° C; Curve (c): 2½ potentiodynamic cycles, 20 mV s^{-1}, in the same electrolytes as (b).

insertion of the corresponding charges, Q, into the relationship

$$y = \frac{2Q_{E,0}}{Q_0 - Q_{E,0}} \quad (1)$$

Reversible potentiodynamic cycling of the polypyrrole layer can be achieved in the acetonitrile electrolyte, as may be seen from Fig. 6. The current voltage curves closely resemble those measured with platinum as a substrate. The anodic current maximum is shifted in the negative direction. In the case of iron, remarkable differences were observed previously [12]. However, all attempts to cycle the polypyrrole layer in the oxalic acid itself failed totally. No recharging of the undoped layer was possible. This finding corresponds to the general rule for polypyrrole that carboxylic acid anions are not suitable as dopants [26]. But it contradicts the possibility of inserting CF_3COO^- anions, which is due to its higher acidity constant [26, 27], for oxalic acid has a large first acidity constant. Steric effects may play a rôle in this case.

3.6. *Copper plating*

The copper plating of aluminium has some inherent problems due to the presence of an unreducable oxide layer covering the metal substrate. Pretreatment of the Al with a zincate bath has been recommended among others [28]. We found that well-adhering copper layers could be electrodeposited on Al, anodically precoated with a thin polypyrrole layer. Table 4 complies some of our typical results.

The copper deposit is irregular (localized growth leads to an inhomogeneous, imperfect coating) if the Al is untreated or if the PPy is relatively thin (entries 1 and 3, respectively). However, a homogeneous perfect coating of PPy is accomplished in the case of thicker PPy precoatings (as for entries 2 and 4). The overvoltage is about 0.5 V, and this is characteristic for a high local current density. Nevertheless, the copper film is relatively smooth. Microscopic inspection of the mechanically detached metal coating discloses a polypyrrole layer adhering at the backside of the copper foil. This indicates that the polypyrrole adheres relatively strongly to the copper layer.

3.7. *Impedance spectroscopy*

Impedance measurements in the frequency range 10^{-1}–10^5 s^{-1} were performed to aquire further information about the composition of the Al/oxide/(polypyrrole) system. Our results are represented in Figs 7a and b and 8 as typical Nyquist plots. Table 5 provides an evaluation of these plots in terms of the equivalent

Table 4. Electrodeposition of Cu on Al, anodically precoated with PPy. PPy: j = 1 mA cm^{-2}, 0.8 M Py/0.1 M $H_2C_2O_4$, 0° C. Cu: j = 25 mA cm^{-2}, 0.25 M $CuSO_4$, 20° C

No.	*Al-Pretreatment*	*Al-Precoating with PPy d_n (μm)*	*Electrodeposition of Cu*			*Quality of Cu-coating*
			c.e. (%)	*U_{SSCE} (V)*	*d (μm)*	
1	–	–	96	−500	5.0	irregular
2	PD	10	96	−460	7.6	regular
3	GA	1	96	−460	6.0	irregular
4	GA	3	96	−460	7.6	regular

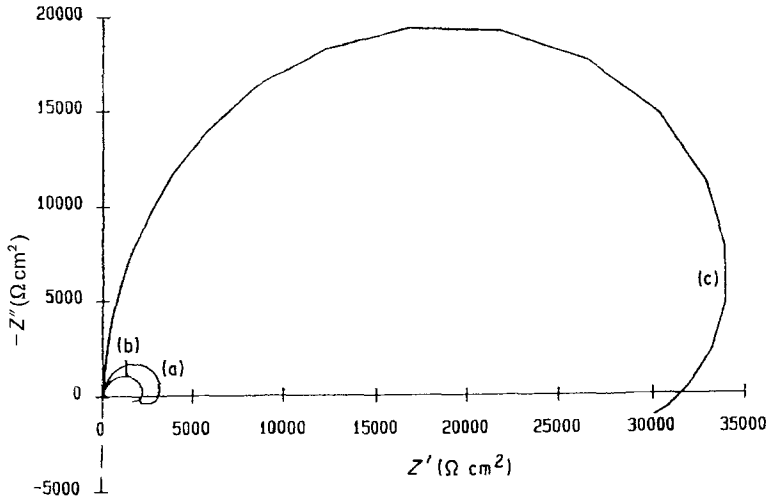

Fig. 7a. Nyquist plots for aluminium electrodes, $A = 4\,cm^2$, in 0.1 M aqueous $H_2C_2O_4$. Frequency range $10^{-1}-10^5\,s^{-1}$. The electrode was at the restpotential: -0.35 V with respect to SHE. Curve (a): anodic pretreatment 'GA', $j = 24\,mA\,cm^{-2}$ in 0.1 M HNO_3/0.1 M pyrrole for 2 minutes; Curve (b): mechanical pretreatment 'PD'; Curve (c): without pretreatment.

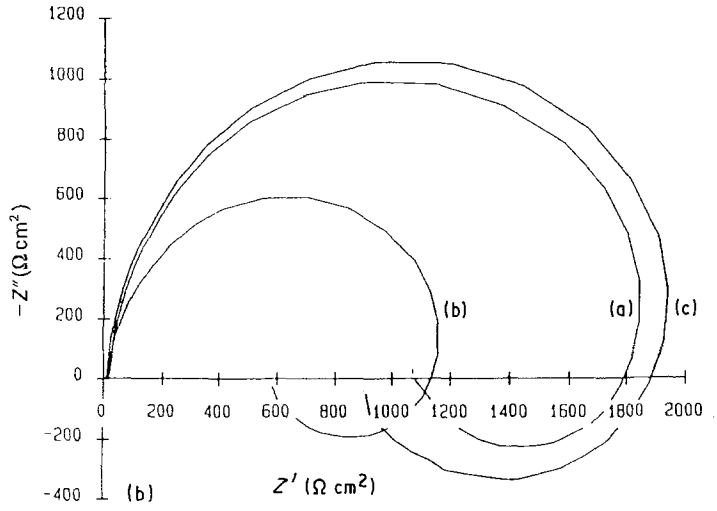

Fig. 7b. The same as Fig. 7a, but with an anodic polarization of the electrode to the potential of polypyrrole formation, $+0.83$ V with respect to SHE.

circuits represented in Figs 9a and b. Al-electrodes with a variety of compositions, chemical and anodic pretreatments and 'sealing' conditions have already been characterized via impedance spectroscopy by several researchers [29–33]. Our results for bare Al-electrodes are in qualitative agreement with their results (cf. Fig. 7). Two semicircles for the R_pC-part (negative sign) and the R_lL-part (positive sign) of the equivalent circuit (Fig. 9a) are found. The polarization resistance, R_p, is in the order of 10^3–$10^4\,\Omega cm^{-2}$, as previously observed [29–31]; it can be easily derived from the diameter of the semicircles in Fig. 7 and must be discussed in terms of a polarization resistance for the somewhat undefined charge transfer reaction at

Table 5. Impedance measurements of $Al/Al_2O_3/(PPy)$ electrodes. Evaluation of Nyquist plots in Figs 7 and 8. Electrolyte in all cases: 0.1 *M oxalic acid in water*

Fig.	*Al-electrode characterization*	$R_p + R_L\ (\Omega cm^2)$		$\omega_{at\,max.}\ (s^{-1})$		$C_D\ (C_L)\ (\mu F\,cm^{-2})$		$L\ (Hy\,cm^2)$	
		−0.35 V	+0.83 V	−0.35 V	+0.83 V	−0.35 V	+0.83 V	−0.35 V	+0.83 V
7a, b (curve a)	Anodically pretreated Al according to GA	3320	1870	63	125	4.6	4.0	271	88
7a, b (curve b)	Mechanically pretreated Al according to PD	2220	1160	31	125	14.6	6.6	348	72
7a, b (curve c)	No special pretreatment	34000	2000	7.9	158	3.2	3.0	–	108
8 (curve a)	Al, GA, (see Fig. 7a), 6 μm PPy	22.6		12540		3.4		–	
8 (curve b)	Al, PD, (see Fig. 7b), 6 μm PPy	40		4990		4.8		–	
8 (curve c)	*Platinum*, 6 μm PPy	–		–		–		–	

Potentials with respect to SHE of the electrodes.
Uncoated Al, (Fig. 7): -0.35 V = o.c.p. and $+0.83$ V, electrodeposition potential of PPy.
PPy coated Al, (Fig. 8): $+0.42$ V (o.c.p. at PPy).

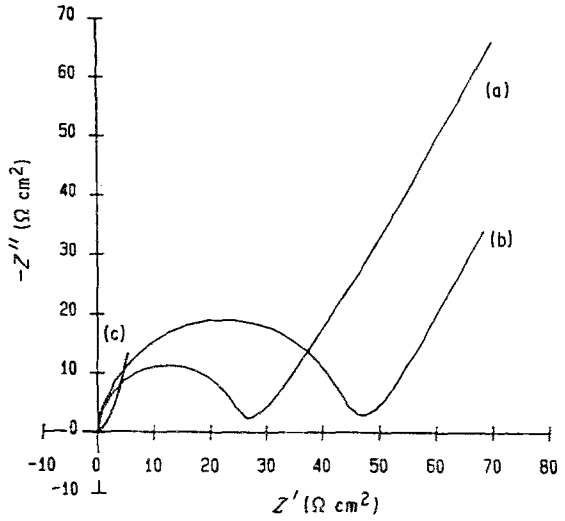

Fig. 8. Nyquist plots for impedance measurements at aluminium electrodes coated with polypyrrole, $A = 4\,\text{cm}^2$, in 0.1 M aqueous $H_2C_2O_4$. Frequency range: $10^{-1}-10^5\,\text{s}^{-1}$. The electrode was at the rest potential: +0.42 V with respect to SHE. A 6 μm PPy layer was electrodeposited from 0.1 M $H_2C_2O_4$/0.8 M pyrrole. Curve (a): anodic pretreatment 'GA', $j = 24\,\text{mA cm}^{-2}$, in 0.1 M HNO_3/0.1 M pyrrole for 2 minutes; Curve (b): mechanical pretreatment 'PD'; Curve (c): smooth platinum.

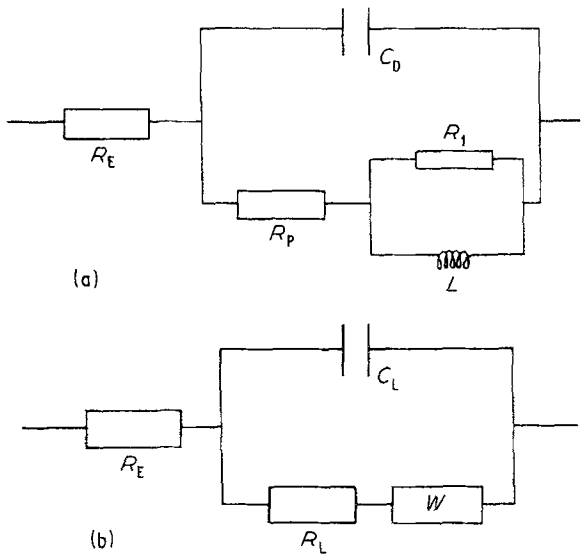

Fig. 9. Equivalent circuits for aluminium electrodes: Circuit (a) for Al/Al_2O_3: C_D = double layer capacity, R_E = electrolyte resistance, R_P = polarization resistance, R_1L = resistance-inductance combination. Circuit (b) for Al/Al_2O_3/PPy: C_L = capacity of intermediate layer, R_L = resistance of intermediate layer, R_E = electrolyte resistance, W = Warburg impedance.

the active surface of the aluminium electrode. The real meaning of the low frequency inductive part is not yet clear, but it may be understood in terms of a corrosion process, where cathodic hydrogen evolution is superimposed on the anodic Al dissolution. Fig. 7a holds for the open circuit potential (o.c.p.) behaviour in the slightly corrosive electrolyte (0.1 M $H_2C_2O_4$). The rest potential is about -350 mV with respect to SHE. Fig. 7b is the result for impedance measurements at the anodically polarized electrode. The potential was +830 mV vs SHE corresponding roughly to that potential, established in the course of electrodeposition of polypyrrole on the aluminium. This reflects the anodic dissolution of Al in the early stages of the PPy deposition, when the coverage of the electrode with the polymer is not yet complete.

Under these conditions R_p decreased according to the increasing slope of the current-voltage curve. The capacity is in the order of the double layer capacity (cf. Table 5), multiplied by the degree of coverage for the active surface sites, which is of the order of 10% (see § 4). C_A was calculated from the simple relationship

$$C_A = \frac{1}{\omega_{(\text{at max.})}\, R_A} \tag{2}$$

where $\omega_{\text{at max}}$ corresponds to the frequency at the maximum of the semicircle and R_A to R_p or R_L. C_A is in close agreement with values found by application of an appropriate computer programme [34]. Some contribution of the capacity of a very thin Al_2O_3-layer, in series with C_D, may also play a role [31].

The impedance behaviour for the Al-electrodes electrocoated with a 6 μm PPy-layer is quite different (cf. Fig. 8). The RC semicircle shrank by two to three orders of magnitude to some 10 ohms, and the inductive part was replaced by some kind of Warburg impedance. The latter part is due to the limited mobility of the anions in the solid ($D \approx 10^{-10}\,\text{cm}^2\,\text{s}^{-1}$, cf. [35]). The semicircle is now representative of the interlayer PPy/Al_2O_3 between Al and PPy (cf. Fig. 10). The situation resembles a capacitor ('metal' plated Al and doped PPy) with a composite material Al_2O_3/PPy as a non-ideal dielectric in between. The Al_2O_3 pores are filled with the electronic conductor PPy rather than with the electrolyte. If one calculates the overall resistance of the combined PPy layer according to the pore model outlined in § 4, the result is 6 orders of magnitude too low with respect to the measurement of R_A. The calculation for the composite part PPy/Al_2O_3 was performed using the expression

$$R_A = \frac{\rho L}{\Theta} \tag{3}$$

where ρ is the resistivity of the polypyrrole (ρ = 0.1 Ω cm), L is the length of the pores and Θ is the degree of coverage for the PPy filled pores which is, for both models, ~7–8% (see Fig. 10). The only way to understand this large discrepancy is to assume a much higher resistivity for that PPy part which fills the pores. This is a reasonable assumption due to the fact that this part is electrodeposited at high local current densities, leading to an overoxidized polypyrrole with a resistivity in the order of $10^6\,\Omega$cm. Some contribution of the Al_2O_3 itself to the electronic contact may arise under these conditions. The capacitive part indicates a value which is due to the capacity of the 'combined interlayer', contacted at both sides with the electronic conductors Al and PPy (see Table 5). If we use the expression

$$C_A = \frac{\varepsilon\varepsilon_0}{L} \tag{4}$$

assuming L = 100 nm and ε = 8 (Al_2O_3), C_A would

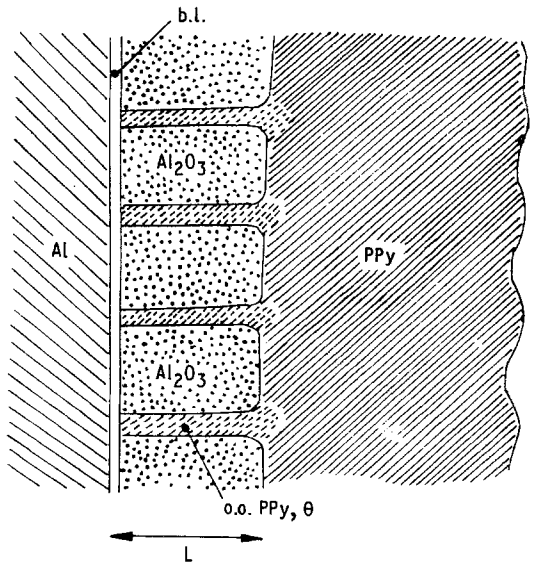

Fig. 10. Cross-sectional view of a sandwich $Al/Al_2O_3/PPy$, which can be described as a capacitor. b.l. = barrier layer, o.o. PPy = overoxidized polypyrrole.

be $\sim 0.1\,\mu F\,cm^{-2}$. A possible explanation for this kind of discrepancy would by an unusually high permittivity number, ε, for the composite dielectric 'Al_2O_3/overoxidized PPy', sandwiched between the 'plates' of Al and PPy. Additionally, the capacity of a thin Al_2O_3 barrier layer may be of some influence.

The electrochemical charge transfer at the phase boundary PPy/electrolyte appears to be quite reversible, and the corresponding measurements at a PPy/Pt-electrode lead to a very small semicircle (curve c in Fig. 8). As mentioned above, the low frequency part in all three cases must be expressed as a Warburg impedance in terms of slow diffusion of counterions in the solid, and a thorough analysis of these features is available in the literature [36, 37]. In all three cases, this low frequency part ends at $31\,s^{-1}$.

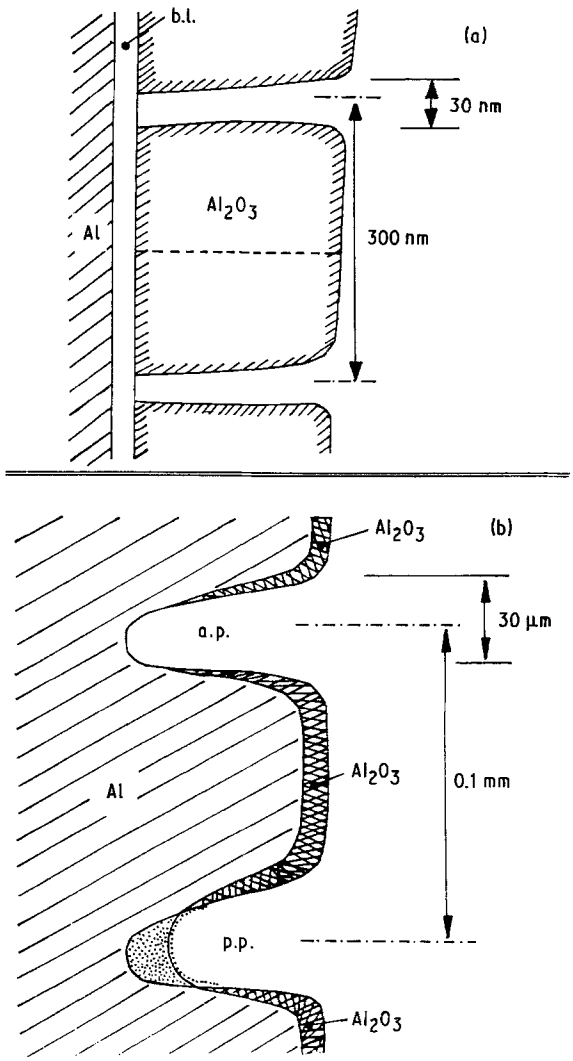

Fig. 11. Cross-sectional view of two types of porous Al_2O_3 layers on Al, schematically, b.l. = barrier layer (n-Al_2O_3). Diagram (a): ALCOA model, about 10^{10} pores cm^{-2} [15, 16]. Diagram (b): pitted Al electrode, about 10^4 pores cm^{-2} [17–21]. a.p. = active pit, p.p. = passive pit.

4. Conclusions

The electrochemical behaviour of Al in aqueous electrolytes is characterized by the presence of an Al_2O_3 layer with the well known duplex structure [15, 16]. It cannot be cathodically reduced under these conditions, but it chemically dissolves at extreme pH values. Pores in the Al_2O_3 layer play an important role. The pores in the Alcoa model (duplex layer) are very small, with diameters 1.5 – 3 nm, nevertheless they provide an initial current path for any electrochemical process. The electrodeposition of polypyrrole must start in these pores. The schematic representation in Fig. 11a leads to a pore density of 8% with respect to the geometric surface area of the electrode. An appropriate pretreatment of the Al is essential for the electrodeposition of a coherent, well adhering PPy layer.

A second type of pore is generated in electrolytes such as 0.1 M HNO_3 by anodic pitting. These pores are much larger by three orders of magnitude. A typical diameter is $30\,\mu m$, and they can be recognized in the microscope In the presence of pyrrole, electrodeposition of polypyrrole is directly identified in the pores. The pore density can be calculated from the geometry disclosed in the micrograph, and leads to a value of 7%, which is close to that of the former model. Thus, the geometrical current density is amplified by a factor of about ten in the pores. This leads clearly to an overoxidized PPy product [38], and a dramatic loss in electronic conductivity can be expected. This was detected with the help of impedance measurements, (cf. §3.8). The sandwich Al/Al_2O_3 + overoxidized PPy/PPy layer can be regarded as a capacitor with two conducting 'plates', Al and a layer of doped PPy, and a specialized dielectric in between (cf. Fig. 10). Our impedance measurements disclose that this dielectric represents a very high pemittivity number of magnitude 10^3. This could be of interest for the development of a microcapacitor. The resistivity of $10^6\,\Omega\,cm$ of the overoxidized polypyrrole filling the pores does not lead to excessive *IR* (potential drop) due to the pore dimensions and the low currents.

If we focus finally on electrochemical surface

techniques, the three most attractive *aqueous* electrolytes for the electrodeposition of PPy on Al are acids, namely, HNO_3, H_2SO_4, and $H_2C_2O_4$. The tendency for the deposition of a well-adhering PPy *layer* increases from left to right. Oxalic acid was recently identified in our laboratory as an electrolyte which also leads to extremely adherent PPy layers on *iron*. On the other hand, the tendency for polypyrrole *powder* deposition increases from right to left, and HNO_3 is very specific under special conditions [24, 25]. If these acids are involved, a combination of anodic pitting (HNO_3), or anodic thickness growth of the Al_2O_3 layer ($H_2C_2O_4$, H_2SO_4) with the electropolymerization process itself, is observed [15–21]. Only after a full blocking of the pores by electrogenerated PPy, is the anodic corrosion of the Al totally inhibited. The polypyrrole deposition in the pits may serve as a new probe for investigation of pitting processes on aluminium.

Acknowledgements

We are indebted to AIF (Arbeitsgemeinschaft Industrieller Forschungsvereinigungen) and to GIF (German Israeli Foundation) for financial support of our work.

References

[1] A. Angeli, *Gazz. Chim. Ital.* **46** II (1916) 279, **48** II (1918) 21.
[2] G. P. Gardini, *Adv. Heterocycl. Chem.* **15** (1973) 67.
[3] R. Steude, PhD thesis July 1933, Technische Hochschule, Munich.
[4] A. Dall'Olio, Y. Dascola, V. Varacca and V. Bocchi, *C.R. Acad. Sci.*, Ser. C, **267** (1968) 433.
[5] A. F. Diaz and J. I. Castillo, *J. Chem. Soc. Chem. Commun.* (1980) 397.
[6] A. F. Diaz, *Chemica Scripta* **17** (1981) 145.
[7] G. Wegner, *Angew. Chem.* **93** (1981) 352, *Angew. Chem. Internat.* **20** (1981) 361.
[8] T. A. Skotheim (Ed), Handbook of Conducting Polymers', Vols. 1 and 2, Marcel Dekker, New York (1986).
[9] J. Heinze, *Tropics in Current Chemistry* **191** (1989), in press.
[10] J. Prejza, I. Lundström and T. Skotheim, *J. Electrochem. Soc.* **129** (1982) 1685.
[11] K. M. Cheung, D. Bloor and G. C. Stevens, *Polymer* **29** (1988) 1709.
[12] M. Schirmeisen and F. Beck, *J. Appl. Electrochem.* **19** (1989) 401.
[13] P. Hülser and F. Beck, *J. Electroanal. Chem.*, in press.
[14] F. Beck and H. Schulz, *Ber. Bunsenges. Phys. Chem.* **88** (1984) 155.
[15] F. Keller, M. S. Hunter and D. L. Robinson, *J. Electrochem. Soc.* **100** (1953) 411.
[16] P. A. Malachesky, in 'Encyclopedia of Electrochemistry of the Elements', (edited by A. J. Bard), Marcel Dekker, New York (1976).
[17] U. R. Evans, 'Conference on Localized Corrosion', Williamsburg (1974) (edited by R. W. Staehle, J. Kruger and B. F. Brown), NACE, Houston (1974).
[18] 'Proceed. 4th Internat. Symp. Passivity' (Airlie), 1977, (edited by R. P. Frankenthal and J. Kruger), The Electrochem. Soc., Princeton (1978).
[19] H. Kaesche, 'Die Korrosion der Metalle', Springer, Berlin (1978), (Corrosion of Metals, NACE, Houston 1986).
[20] M. Baumgärtner and H. Kaeshce, *Corros. Sci.* **29** (1989) 363.
[21] D. M. Drazic, S. K. Zecevic, R. T. Atanowski and A. R. Despic, *Electrochem. Acta* **28** (1983) 751.
[22] S. Asavapiriyanont, G. K.Chandler, G. A. Gunawardena and D. Pletcher, *J. Electroanal. Chem.* **17** (1984) 229.
[23] M. Oberst and F. Beck, *Electrochim. Acta*, submitted.
[24] F. Beck and P. Hülser, German Patent Application 3906563.4 (2.3.1989).
[25] F. Beck and P. Hülser, *J. Electrochem. Soc.*, in press.
[26] L. F. Warren and D. P. Anderson, *J. Electrochem. Soc.* **134** (1987) 101.
[27] S. Kuwabata, J. Nakamura and H. Honeyama, *J. Chem. Soc., Chem. Commun.* (1988) 779.
[28] A. F. Bogenschütz, personal communication, also see *Galvanotechnik* **77** (1986) 1575.
[29] J. P. Hoar and G. C. Wood, *Electrochim. Acta* **7** (1962) 333.
[30] R. D. Armstrong and K. Edmondson, *Electrochim. Acta* **18** (1973) 937.
[31] J. Bessone, C. Mayer, K. Jüttner and W. J. Lorenz, *Electrochim. Acta* **28** (1983) 171.
[32] J. Hitzig, K. Jüttner, W. J. Lorenz and W. Paatsch, *J. Electrochem. Soc.* **133** (1986) 887.
[33] F. Mansfeld and M. W. Kendig, *J. Electrochem. Soc.* **135** (1988) 828.
[34] J. R. Macdonald and L. D. Potter, Jr., *Solid State Ionics* **23** (1987) 61; J. R. Macdonald, Complex Nonlinear Least Squares Impedance Fitting Programme (CNLS programme).
[35] F. Beck and M. Oberst, *Makromol. Chem., Macromol Symp.* **8** (1987) 97.
[36] J. Tanguy, N. Mermilliod and M. Hoclet, *J. Electrochem. Soc.* **134** (1987) 796.
[37] J. Tanguy, N. Mermilliod and M. Hoclet, *Synth. Metals* **18** (1987) 7.
[38] F. Beck, P. Braun and M. Oberst, *Ber. Bunsenges. Phys. Chem.* **91** (1987) 967.